Cooperative Self-Assembly of Oligo(*m*-phenyleneethynylenes) into Supramolecular Coordination Polymers

Jay Wm. Wackerly and Jeffrey S. Moore*

Departments of Chemistry and Materials Science and Engineering, Roger Adams Laboratory, University of Illinois at Urbana−Champaign, Urbana, Illinois 61801

Received June 14, 2006; Revised Manuscript Received August 7, 2006

ABSTRACT: Here we report the supramolecular coordination polymerization of four bis-functionalized phenyleneethynylene oligomers. Each oligomer was terminated with pyridyl end groups; three of them had *meta* backbone linkages and varied in the number of phenyleneethynylene units from four to eight. The fourth oligomer served as a geometric control with *para* connectivity and three phenyleneethynylene units. Upon the addition of *trans*-dichlorobis(acetonitrile)palladium to a solution of oligomer, supramolecular assembly by metal coordination was observed by UV spectroscopy, NMR, and isothermal titration calorimetry. For the tetramer and octamer, the experimental evidence is consistent with a cooperative polymerization mechanism involving pyridine−palladium coordination and π-stacking leading to a helical supramolecular polymer. For the hexamer, macrocyclization followed by columnar aggregation was indicated by the data. In contrast, the *para*-linked control oligomer exhibited noncooperative, isodesmic step-growth polymerization. This work thus demonstrates how the supramolecular polymerization mechanism is sensitive to length of the starting oligomer and geometry of the monomer units.

Introduction

Cooperativity is a pervasive phenomenon among the biomacromolecules and is especially important for functions such as active site binding,[1] protein folding,[2] enzyme activity,[3] protein self-assembly,[4] and transcription,[5] to name a few. Actin and tubulin form filaments[6] and microtubules,[7] respectively, by a supramolecular polymerization process in which globular proteins act as monomers and whose mechanism of growth follows the cooperative nucleation−elongation pathway. This mechanism brings protein molecules together without covalent bonding interactions allowing well-balanced assembly and disassembly, dynamic behavior that translates directly into useful functions. Despite the abundance of these natural examples, few synthetic systems have been shown to exhibit polymer growth by the nucleation−elongation pathway.[8,9] Herein we report a synthetic nucleation−elongation polymerization governed exclusively by noncovalent interactions.

Synthetic noncovalent, or supramolecular, polymers have garnered a great deal of attention recently.[10−13] Indeed, some synthetic supramolecular polymers have shown cooperativity through hydrogen bonding[14] or both hydrogen bonding and π-stacking.[15,16] The same cannot be said about polymerizations employing coordination bonds.[17−21] A coordination polymer exhibiting π-stacking has been recently studied in the solid state, but the polymerization mechanism was not discussed.[22] In this article we describe the synthesis and characterization of three *m*-phenyleneethynylene (*m*PE) oligomers (**1**−**3**) that, depending on the oligomer length, either form helical (Figure 1A) or tubular (Figure 1B) supramolecular coordination polymers with π-stacking interactions upon the addition of palladium in acetonitrile.

Previous work from our laboratory has shown that when 2 equiv of *m*PE oligomers terminated at one end with a coordinating pyridine group are added to a solution of *trans*-dichlorobis(acetonitrile)palladium, the oligomers self-assemble into a helical conformation driven by the cooperativity of metal−ligand binding and π-stacking.[23] We thought that by functionalizing both ends and varying the length of the oligomers new and unique supramolecular polymers would result by an interesting polymerization mechanism. Changing the geometry of the oligomer backbone from *meta* to *para* should also change the mechanism of polymerization, since the *para* geometry is incapable of adopting a helical conformation.

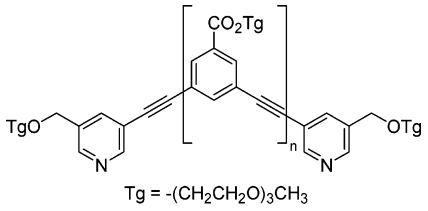

1: n=2
2: n=4
3: n=6

Studies of *m*PE oligomers have demonstrated that they adopt a helical conformation with six units per turn stabilized by $\pi-\pi$ interactions in polar solvents.[24−26] These *m*PE oligomers have been termed foldamers, compounds that adopt a conformationally ordered state in solution.[27−32] One unique aspect of *m*PE oligomers is that they will not fold until a critical chain length is achieved.[33] We have also shown that *m*PE oligomers with specialized end groups exhibit interesting dynamic covalent characteristics.[23,34−38] In one such study, short length *m*PE oligomers containing imine end groups were driven to form high molecular weight polymers through a nucleation−elongation mechanism by taking advantage of dynamic covalent imine metathesis.[37]

Nucleation−elongation polymerization results when the initial oligomerization of monomers is energetically disfavored (nucleation) relative to a favorable polymerization (elongation). This generally leads to the predominance of either high molecular weight polymer or monomer species (sometimes both) and minimal oligomers of intermediate length, which is in great contrast to typical step-growth isodesmic polymerizations.[39] The thermodynamically favored elongation steps arise from noncovalent interactions between two nonadjacent monomers, once

* Corresponding author. E-mail: jsmoore@uiuc.edu.

10.1021/ma061331k CCC: $33.50
Published on Web 09/22/2006

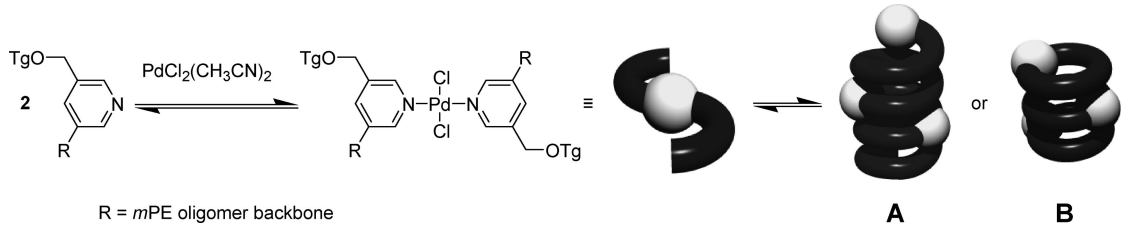

Figure 1. Palladium−pyridine binding to form a metal−ligand complex followed by subsequent "monomer" additions to form a supramolecular foldamer (A) or a π-stacked columnar polymer (B).

Scheme 1. Formation of Supramolecular Polymers from Oligomers 1−3

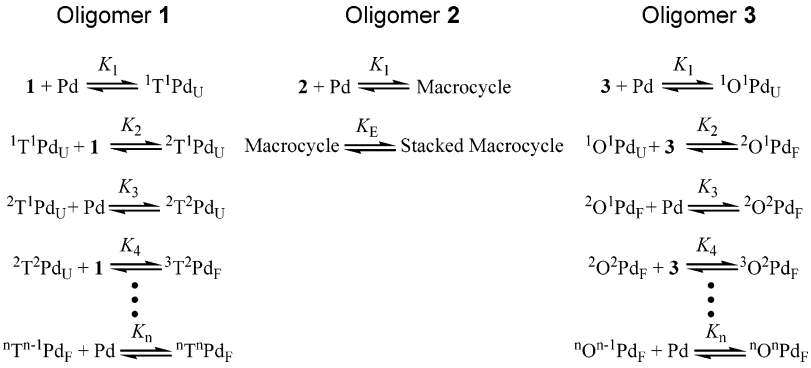

Scheme 2. Synthesis of Terminal Monomer Unit 7[a]

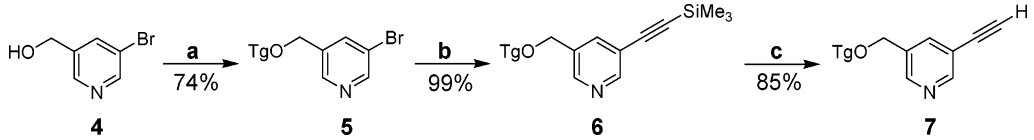

[a] Reagents and conditions: (a) TgOTs, KOH, DMSO, 60 °C; (b) trimethylsilylacetylene, $PdCl_2(PPh_3)_2$, CuI, Et_3N, 80 °C; (c) TBAF, THF.

Scheme 3. Synthesis of Tetramer 1[a]

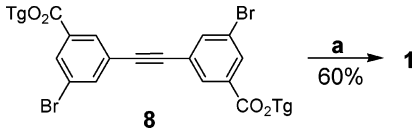

[a] Reagents and conditions: (a) **7**, Pd(P*t*-Bu$_3$)$_2$, CuI, Et_3N, 75 °C.

the polymerization reaches a critical chain length.[8] Because a critical chain length (usually ca. 10 *m*PE units for foldamers) must be attained before folding occurs, oligomers **1**−**3** might undergo nucleation−elongation polymerization in the presence of palladium since they start in an unfolded state below the critical chain length and should be folded above it (Figure 1A).

Hypothetical models for nucleation−elongation polymerization of the various oligomers investigated here are shown in Scheme 1, where the superscript represents the degree of polymerization of the starting oligomers (i.e., T = tetramer **1** and O = octamer **3**) and the trailing subscript represents whether the polymer is below (unfolded, U) or above (folded, F) the critical chain length. An association event, defined as palladium−pyridine coordination where either the palladium or pyridine is part of the polymer backbone, that involves the interaction of unfolded chains is considered a nucleation event when no stabilization from π-stacking interactions is gained. An association event that involves a folded chain and a starting oligomer is considered an elongation event because folding contributes to the stability of the associated oligomers. Tetramer **1** must undergo four nucleation events (K_1−K_4) before the critical chain length is reached, at which point elongation occurs (K_5−K_n). Octamer **3**, on the other hand, only requires two nucleation events (K_1−K_2) before elongation occurs (K_3−K_n). On the basis of previous studies of imine-linked oligomers, we predicted that hexamer **2** would form a macrocycle rather than a polymer (Scheme 1).[35] Shape-persistent arylene ethynylene macrocycles have the ability to π-stack into columner aggregates in certain solvents.[40] In the presence of palladium, hexamer **2** may preferentially form a macrocycle (K_1) because its length is suitable to form an unstrained cyclic. The smaller size of the macrocycle compared to a supramolecular polymer may make this the thermodynamically favored product for entropic reasons.[41] Moreover, the flat macrocycle should possess the ability to form π-stacked columnar aggregates (Figure 1B), presumably by an indefinite isodesmic process governed by the association constant (K_E).[42]

The equilibria described for oligomers **1**−**3** in Scheme 1 have analogues in protein assembly. For example, certain proteins form macrocycles in order to perform their functions.[43] The heat shock protein GroEL forms a heptameric macrocycle which creates a 45 Å diameter cavity which aids in folding of other proteins.[44] The requirement of supramolecular polymerization to perform a specific function is illustrated by actin and tubulin.[45] Furthermore, the tobacco mosaic virus can alter its intermolecular interactions (a combination of π-stacking, metal−ligand bonding, and hydrogen bonding) to undergo a macrocycle-to-helix transformation.[46] Inspired by nature's cooperative supramolecular assemblies, we sought to mimic this balance between macrocycle formation and supramolecular polymerization. We report the reversible formation of three types of supramolecular polymers; the operative mechanism is found to be sensitive to oligomer length and backbone geometry.

Results and Discussion

Synthesis. In our previous report of monopyridine-functionalized oligomers there was no solubilizing side chain on the

Scheme 4. Synthesis of Hexamer 2 and Octamer 3[a]

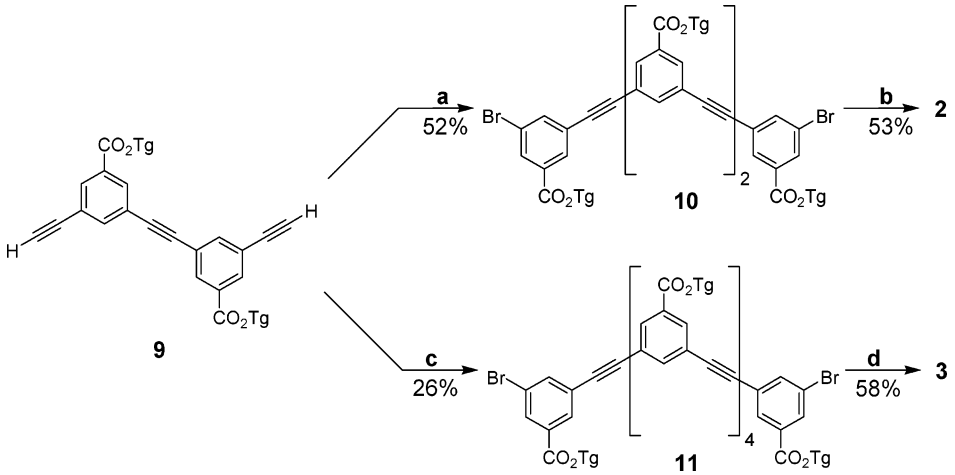

[a] Reagents and conditions: (a) 2-[2-(2-methoxyethoxy)ethoxy]ethyl 3-bromo-5-iodobenzoate, $PdCl_2(PPh_3)_2$, CuI, Et_3N, rt; (b) **7**, $Pd(Pt\text{-}Bu_3)_2$, $ZnBr_2$, Et_3N, rt; (c) **8**, $Pd_2(dba)_3$, CuI, Et_3N, 70 °C; (d) **7**, $Pd(Pt\text{-}Bu_3)_2$, CuI, Et_3N, 70 °C.

terminal pyridine unit.[23] Preliminary studies indicated that the supramolecular polymers targeted here would require additional groups to enhance the solubility. To this end, a triethylene glycol chain was added to the pyridine unit of oligomers **1**−**3**. The synthesis of the pyridine-terminated *m*PE oligomers began with the preparation of the terminal ethynylpyridine monomer unit (Scheme 2). Alcohol **4** was reacted with triethylene glycol monomethyl tosylate to yield ether **5**, which was then coupled to trimethylsilylacetylene to give alkyne **6**. Treatment with tetrabutylammonium fluoride (TBAF) gave the ethynylpyridine end group **7**.

The synthesis of *m*PE dimer **8** has been previously described.[35] Tetramer **1** (Scheme 3) was synthesized by coupling **8** with 2 equiv of **7**. Dimer **9**, the synthesis of which has been previously described,[35] was a key intermediate since it was a precursor for both hexamer **2** and octamer **3** (Scheme 4). Coupling **9** with 2 equiv of 2-[2-(2-methoxyethoxy)ethoxy]ethyl 3-bromo-5-iodo-benzoate gave tetramer **10**, which was then coupled with 2 equiv of ethynylpyridine **7** to afford the desired hexamer **2**. Alternatively, coupling of **9** with 5 equiv of **8** gave hexamer **11**, which was subsequently coupled with 2 equiv of ethynylpyridine **7** to afford the desired octamer **3**.

Complex Formation: Physical Appearance and MS Analysis. The supramolecular palladium complexes were prepared by adding 1 equiv of *trans*-dichlorobis(acetonitrile)-palladium to a solution of oligomer **1**, **2**, or **3** in acetonitrile. A change in the physical appearance of each oligomer was noticed upon the addition of the palladium and removal of the solvent. Tetramer **1** changed from an oil to a yellow waxy solid. Hexamer **2** changed from a waxy solid to a yellow sticky spongelike solid. Octamer **3** changed from a waxy solid to a yellow rigid solid. Starting from a solution of the supramolecular complex, the pure oligomer could be recovered by addition of excess PPh_3 and subsequent column chromatography.

MALDI mass spectrometry of these products revealed some differences between the oligomers. Though the most intense peak observed in the spectrum of hexamer **2** with palladium correlated to free hexamer, a significant peak corresponding to the mass and isotopic distribution of **2**·$PdCl_2$ was observed (Figure 2). Conversely, when tetramer **1** and octamer **3** were combined with 1 equiv palladium and analyzed by MALDI, only the free oligomer was observed, supporting the idea that **1** and **3** form a different type of structure than **2**.

UV Spectroscopy. For *m*PE oligomers, we have previously shown that the absorbance at 303 nm is dependent upon the

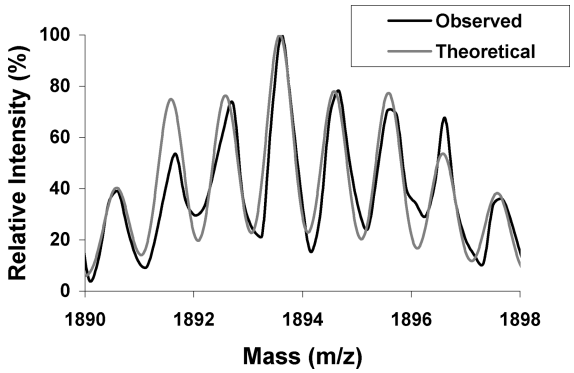

Figure 2. MALDI-TOF MS of a mixture of hexamer **2** and 1 equiv of palladium (M + Na, m/z = 1893.6). The observed spectrum is shown in black, and the calculated isotopic distribution is shown in gray.

conformation of the oligomer backbone.[23−25,47] When *m*PE oligomers adopt a highly *cisoid* conformation (i.e., helix or macrocycle), the absorbance at 303 nm is significantly attenuated relative to the peak at 280 nm. It can be seen in Figure 3 that a significant decrease in the 303 nm peak occurs for oligomers **1**−**3** upon the addition of palladium in an acetonitrile solution, thus indicating that a predominately *cisoid* conformation has formed.

To probe the oligomer−palladium stoichiometry for each of the complexes, the method of continuous variation (Job's method) was employed.[48,49] The samples were analyzed in acetonitrile at 25, 20, and 10 μM concentrations of **1**, **2**, and **3**, respectively, by varying concentrations of palladium while keeping the concentration of oligomer + palladium constant. The normalized absorbance at 303 nm was calculated according to eq 1.

$$\text{normalized absorbance} = -(A - \epsilon_P b P_T - \epsilon_O b O_T) \quad (1)$$

The measured absorbance (A), cell path length (b), the molar absorptivity of pure *trans*-dichlorobis(acetonitrile)palladium (ϵ_P), the molar absorptivity of pure oligomer (ϵ_O), the total concentration of *trans*-dichlorobis(acetonitrile)palladium in solution (P_T), and the total concentration of oligomer in solution (O_T) are all utilized to determine the normalized absorbance.[49] Figure 4 shows that the maximum for each oligomer occurs at 0.5 mole fraction, indicative of a 1:1 palladium:oligomer stoichiometry.[50]

NMR Spectroscopy. An NMR study was undertaken to investigate the species present in solution as palladium was

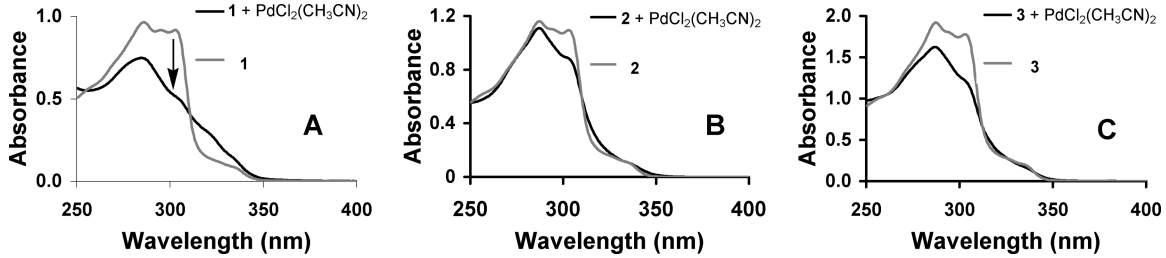

Figure 3. UV spectra of **1** (A), **2** (B), and **3** (C) and a 1:1 mixture of each oligomer with *trans*-dichlorobis(acetonitrile)palladium in acetonitrile (the concentration of **1**, **2**, and **3** in both spectra is 12.5, 10.0, and 10.0 μM, respectively). The decrease in absorbance at 303 nm is shown by the arrow in (A).

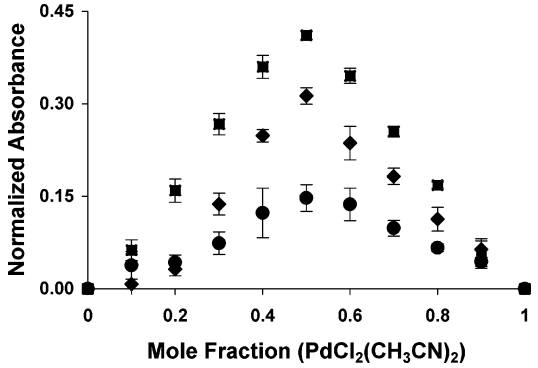

Figure 4. Job's plot in acetonitrile of oligomers **1** (■) at 25 μM, **2** (●) at 20 μM, and **3** (◆) at 10 μM as measured by the normalized absorbance at 303 nm vs the mole fraction $[PdCl_2(CH_3CN)_2]/([PdCl_2(CH_3CN)_2] + [\text{oligomer}])$ at constant $[PdCl_2(CH_3CN)_2] + [\text{oligomer}]$. Error bars were generated from the standard deviation obtained from four measurements of each point.

added. Evidence for folding of oligomers **1** and **3** was observed upon titrating a 1.85 mM solution of each oligomer with varying mol equiv of *trans*-dichlorobis(acetonitrile)palladium in acetonitrile-d_3 using mesitylene as the internal standard (Figure 5). Titration of the two oligomers showed many similar features. For both **1** and **3** the peaks of free oligomer disappeared, and broad upfield peaks appeared with increasing palladium. These broad upfield peaks are consistent with previous observations of aggregated *m*PE foldamers in acetonitrile.[23,24] The integrated area of the entire aromatic region is constant during the titration of both oligomers. Approximately half of the free oligomer is still present at 0.5 mol equiv of palladium (Figure 6). Also, no 1:2 (oligomer:palladium) complex was observed even when excess palladium was present. This behavior is consistent with a nucleation−elongation supramolecular polymerization. Nucleation−elongation polymerizations are known to exclude excess monomer (i.e., oligomer or palladium) in a manner similar to crystal growth.[8,37] This is in contrast to isodesmic polymerization in which a nonlinear decrease in free oligomer concentration is expected as a function of the palladium:oligomer ratio.[39]

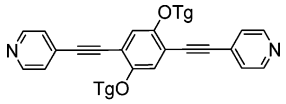

12

In an effort to provide further evidence that conformational ordering is influencing the polymerization of **1** and **3**, oligomer **12** was investigated since its geometry is incommensurate with a helical conformation. Compound **12** links the pyridine unit in a *para* fashion, which only allows the formation of a linear coordination polymer. The triethylene glycol chains on **12** were attached via ether linking groups to decrease self-association by π-stacking.[51] A ^{1}H NMR titration was performed with **12** just as for oligomers **1** and **3**, and the free monomer peaks were integrated relative to the internal standard (Figure 6). Comparison of these data show the linear disappearance of free oligomers **1** and **3** as a function of palladium:oligomer molar ratio, consistent with a theoretical description of nucleation−elongation polymerization (black line, Figure 6).[52] In contrast, **12**

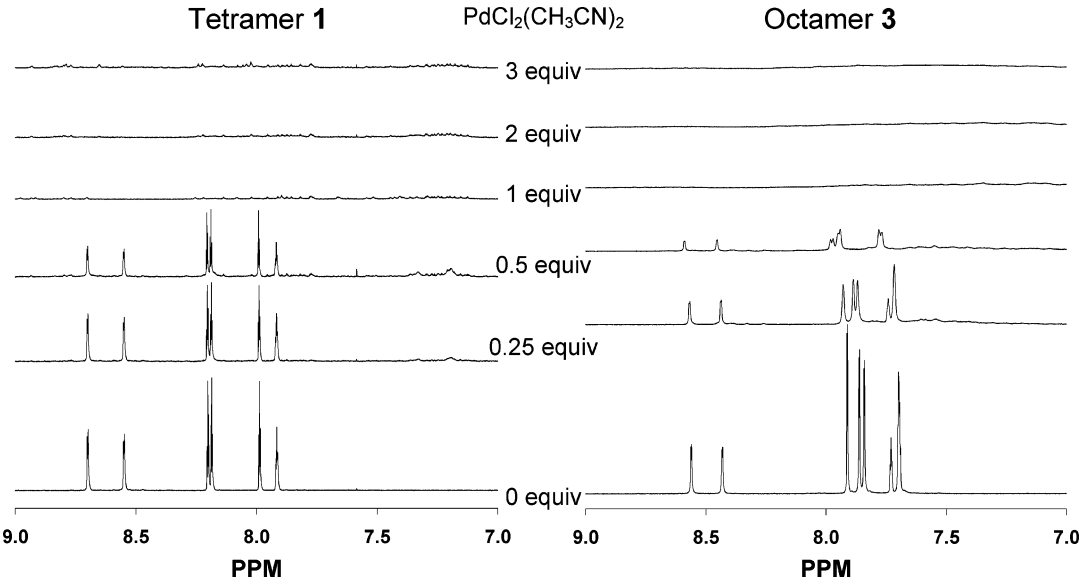

Figure 5. ^{1}H NMR of oligomers **1** and **3** with the indicated equiv of $PdCl_2(CH_3CN)_2$ in acetonitrile-d_6 at an oligomer concentration of 1.85 mM. The intensity of each spectrum was normalized to the mesitylene internal standard present at a concentration of 1.85 mM.

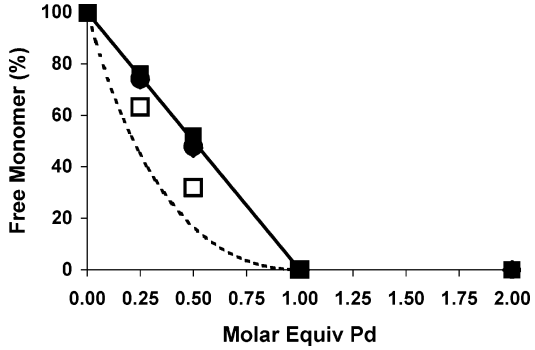

Figure 6. Percentage of free oligomer (**1**, ■; **2**, ●; **3**, ◆; **12**, □) observed by ^{1}H NMR vs mol equiv of the palladium complex. Free monomer was calculated using a mesitylene internal standard and the integration of the aromatic peaks at 0 equiv palladium. The titration was performed three times for control **12**; the data represent the average value with a standard deviation <2% for each point. The soild line represents the expected behavior of cooperative polymerization, and the dashed curve represents the theoretical behavior of step-growth polymerization.[39]

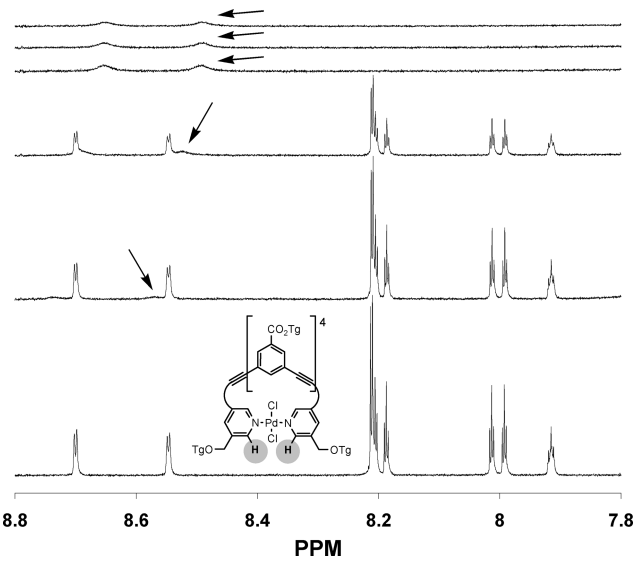

Figure 7. ^{1}H NMR of oligomer **2** with 0 (bottom), 0.25, 0.5, 1, 2, and 3 equiv of $PdCl_2(CH_3CN)_2$ (top) in acetonitrile-d_6 at an oligomer concentration of 0.19 mM. The intensity of each spectrum was normalized to the mesitylene internal standard present at a concentration of 0.19 mM. The arrows denote the peak corresponding to the shaded proton.

deviates from this linear behavior and is in better agreement with an isodesmic step-growth polymerization (Figure 6).[45]

A similar titration with hexamer **2** at a 10-fold lower concentration is shown in Figure 7 where the proton on the pyridine ring at the 2-position is followed. The titration shows the disappearance of free hexamer **2** and appearance of a discrete structure with broadened chemical shifts presumably caused by π-stacking.[53] As expected, the peaks corresponding to the macrocycle shift upfield as palladium is added (vide infra); beyond 1 equiv of palladium the resonances cease to shift. This behavior is consistent with complete formation of a 1:1 palladium:hexamer macrocycle. No destruction of the product (e.g., formation of a 2:1 palladium:hexamer complex) was observed with further increase in palladium. Another titration was also performed in chloroform-*d*, a solvent known to inhibit π-stacking for *m*PE macrocycles.[54] The titration in chloroform shows the formation of discernible peaks shifted downfield of the free hexamer peaks. This shift is expected for a nonaggregated macrocycle formed by pyridine−palladium complexation.[55] The combination of MS, UV, and NMR data are consistent with a macrocyclic structure of the palladium complex from **2**.

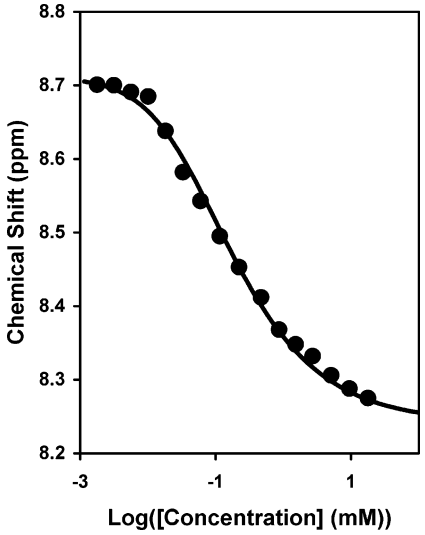

Figure 8. Plot of chemical shift of a pyridine proton (shaded in Figure 7) vs log(concentration) (mM) of an equimolar amount of **2** and $PdCl_2(CH_3CN)_2$ in acetonitrile-d_3 at room temperature. The curve represents the best fit of the data to the isodesmic model of indefinite association when $K_E = 12300 \pm 1400$ M^{-1}.

Next experiments were carried out to quantify the macrocycle self-association. Our laboratory[35,56] and others[57,58] have previously shown that the self-association constant (K_E) of aryleneethynylene macrocycles is well described by the isodesmic model of indefinite association.[42] Using eq 2,[59] it can be seen that the K_E can be determined from an NMR dilution experiment. This was done by plotting the chemical shift of a pyridine proton of the complex formed from hexamer **2** with 1 equiv of *trans*-dichlorobis(acetonitrile)palladium against concentration (Figure 8). From the observed chemical shift (P) at known molar concentrations of the macrocycle (C_T), the chemical shift of free macrocycle ($P_{monomer}$), overall change in chemical shift of free macrocycle to fully stacked macrocycle (Δ), and association constant (K_E) were determined by nonlinear least-squares regression analysis. The K_E in acetonitrile-d_3 was determined to be 12300 ± 1400 M^{-1}. This result is consistent with the observed self-association of *m*PE macrocycles in polar aprotic organic solvents and implies that this metal-coordination macrocycle behaves similarly to previously studied, fully covalent aryleneethynylene macrocycles.[40]

$$P = P_{monomer} - \Delta(1 + (1 - (4K_E C_T + 1)^{1/2})/(2K_E C_T) \quad (2)$$

Isothermal Titration Calorimetry (ITC). ITC was employed to obtain quantitative thermodynamic data for the macrocylization of **2** and the polymerization of **1**, **3**, and **12**. ITC offers the capability to directly determine the enthalpy ($\Delta H°$), and by interpreting the data with a mathematical model for a system of two or more interacting species, the values of equilibrium constants (K_{obs}) can be deduced.[60,61] Since the thermodynamic parameters should be similar for each oligomer with respect to palladium−pyridine binding, the differences in thermodynamic quantities can be attributed to the π-stacking interactions of the complexes. Solutions of oligomers **1**−**3** and **12** were prepared at 0.10 mM concentrations and titrated with a 1.33 mM solution of *trans*-dichlorobis(acetonitrile)palladium in acetonitrile at 20 °C (Figures 9−12). The data were fit using nonlinear least-squares regression analysis to a single-site

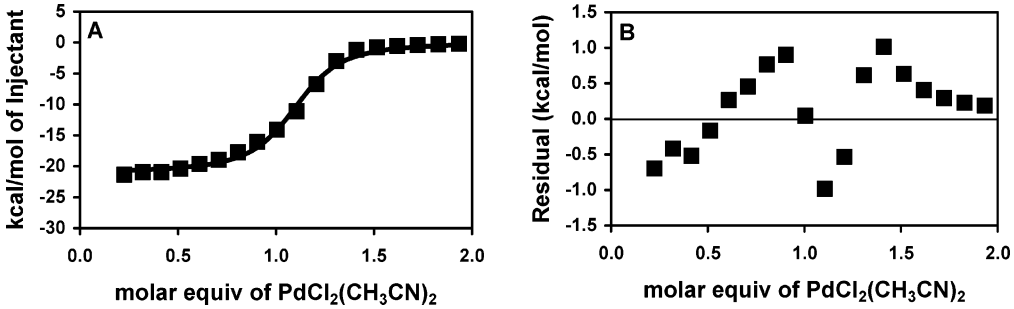

Figure 9. ITC binding isotherm for the titration of a 0.10 mM solution of **1** with a 1.33 mM solution of *trans*-dichlorobis(acetonitrile)palladium in acetonitrile at 20 °C (A). Residual analysis of the difference from the observed data compared to the fit data as a function of palladium (B).

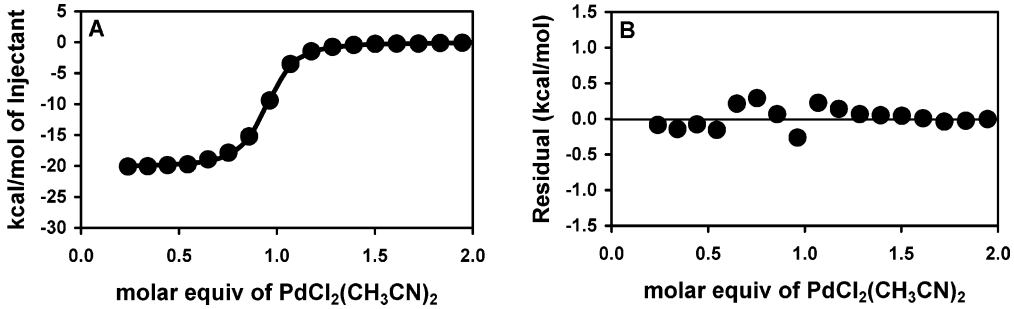

Figure 10. ITC binding isotherm for the titration of a 0.10 mM solution of **2** with a 1.33 mM solution of *trans*-dichlorobis(acetonitrile)palladium in acetonitrile at 20 °C (A). Residual analysis of the difference from the observed data compared to the fit data as a function of palladium (B).

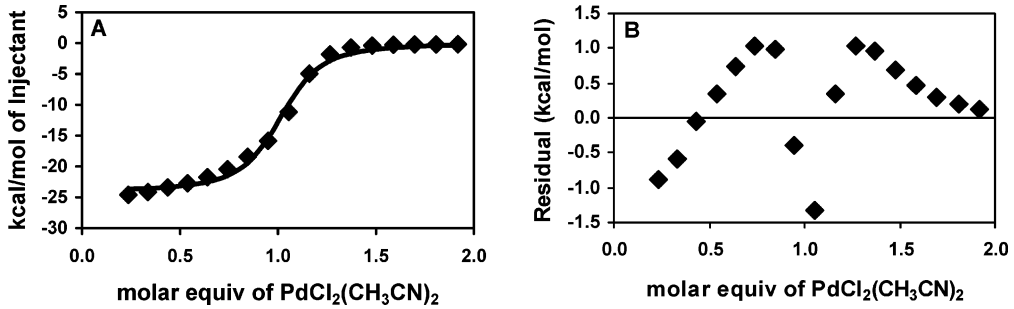

Figure 11. ITC binding isotherm for the titration of a 0.10 mM solution of **3** with a 1.33 mM solution of *trans*-dichlorobis(acetonitrile)palladium in acetonitrile at 20 °C (A). Residual analysis of the difference from the observed data compared to the fit data as a function of palladium (B).

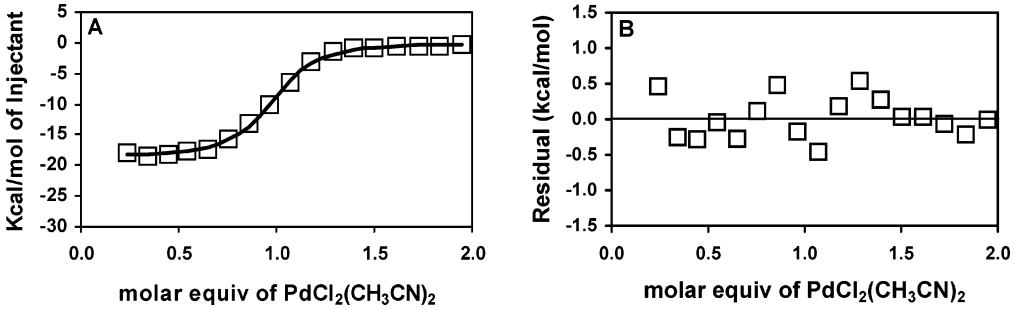

Figure 12. ITC binding isotherm for the titration of a 0.10 mM solution of **12** with a 1.33 mM solution of *trans*-dichlorobis(acetonitrile)palladium in acetonitrile at 20 °C (A). Residual analysis of the difference from the observed data compared to the fit data as a function of palladium (B).

Table 1. Thermodynamic Parameters (in kcal mol^{-1}) for Oligomers 1−3 and 12 Binding to $PdCl_2(CH_3CN)_2$ in Acetonitrile at 20 °C

	1	**2**	**3**	**12**
$\Delta G°$	-7.97 ± 0.12	-8.25 ± 0.03	-8.02 ± 0.08	-7.87 ± 0.06
$\Delta H°$	-21.0 ± 0.2	-20.2 ± 0.01	-24.2 ± 0.3	-17.7 ± 0.1
$T\Delta S°$	-13.0 ± 0.2	-11.9 ± 0.1	-16.2 ± 0.3	-9.8 ± 0.1

binding model (vide infra). After the calculation of K_{obs} and $\Delta H°$, the free energy ($\Delta G°$) and entropy ($\Delta S°$) were determined for the titration of each oligomer (Table 1).

From the data reported above, it is expected that hexamer **2** binds to 1 equiv of palladium with a distinct equilibrium constant (K_{obs}). The model used to describe this behavior (Scheme 1) is consistent with the recorded ITC results. The titration data of hexamer **2** are well described by a single-site binding model with $K_{obs} = (1.35 \pm 0.06) \times 10^6$ M^{-1}. Though K_E must be factored into the K_{obs} value, the fact that the K_{obs} is 2 orders of magnitude larger than the NMR-determined value of K_E indicates that K_{obs} is dominated by the formation of a single macrocycle and not the subsequent π-stacking of the macrocycles. Analysis of residuals shows some systematic error, although not unusually large for treating the data with a two-parameter model (Figure 10).

The titration data for oligomers **1** and **3** are also reasonably well fit by a single-site binding model. Although this treatment is an oversimplification of the polymerization shown in Scheme 1, such behavior would be expected if elongation events in nucleation−elongation polymerizations dominate the K_{obs} value.[62] The K_{obs} for tetramer **1** ($K_{obs} = (8.47 \pm 1.20) \times 10^5$ M^{-1}) showed no statistical difference when compared to octamer **3** ($K_{obs} = (9.10 \pm 0.85) \times 10^5$ M^{-1}). This can be explained by the $\Delta H°$ value for octamer **3** being more enthalpic than **1** because more π-π interactions are obtained from folding per mole of oligomer polymerized; on the other hand, the $\Delta S°$ value is lower for the octamer since it must pay a higher entropic penalty owing to a larger loss of translational degrees of freedom than the tetramer per mole of oligomer. Analysis of residuals for **1** and **3** was nearly identical; both showed systematic error much larger than seen for hexamer **2**, indicating that the single-site binding model does not fully capture this more complex supramolecular process.

Titration data for the control oligomer **12** were well fit by a single-site binding model indicating that each pyridine−palladium coordination was thermodynamically similar. The binding constant for **12** ($K_{obs} = (7.08 \pm 0.61) \times 10^5$ M^{-1}) was the lowest of the oligomers as expected due to the polymerization not being cooperative (i.e., loss of the π-stacking interactions). The titration data for **12** also indicate that coordination-driven polymerization is a favorable process under these conditions. Specifically, the titration is complete at 1 equiv of palladium, and no 1:2 (oligomer:palladium) complex is present when excess palladium is added. Analysis of residuals for **12** only shows random error, indicating that the single-site binding model accurately represents the equilibria.

Interesting enthalpic and entropic differences among the oligomers can be seen from the ITC data in Table 1. Assuming that π-stacking interactions are insignificant for the polymerization of **12**, a ΔH of −17.7 kcal/mol can thus be ascribed to the metal−ligand coordination interactions. Enthalpic changes more negative than −17.7 kcal/mol can be assigned to π-stacking interactions. The $\Delta\Delta H$ for **2** (−2.5 kcal/mol) is smaller than those for **1** and **3** (−3.3 and −6.5 kcal/mol, respectively). Interpreted as π-stacking, these enthalpy values imply a tighter association of the aromatic rings in intramolecular foldamers compared to macrocycles. However, the entropic benefit of macrocycle formation vs polymerization more than compensates for the small enthalpy gain. The combination of enthalpy and entropy values for each oligomer in this study shows that the macrocycle is a little more than 0.2 kcal/mol more favorable than folded polymers from **1** and **3** and almost 0.4 kcal/mol more favorable than a linear polymer from **12**.

Conclusions

Three *m*PE oligomers of slightly different lengths each containing pyridine end groups were synthesized and their coordination polymerizations studied upon adding palladium.[63] Oligomers **1** and **3** were shown to undergo polymerization consistent with a nucleation−elongation mechanism to form supramolecular folded polymers. Hexamer **2** was found to form a shape-persistent macrocycle which then aggregated into a columnar polymer through π-stacking with other macrocycles. Control oligomer **12** with a *para*-linked backbone polymerized by a mechanism consistent with an isodesmic step-growth polymerization. The results indicate that the oligomer length, geometry, and supramolecular interactions directly influence polymerization mechanism. It is apparent from this work that small adjustments of the backbone chain length or angle has a dramatic effect on the structure and mechanism of growth for the supramolecular polymers formed.

These results could be helpful in understanding how and why proteins achieve nucleation−elongation mechanism over macrocyclization (e.g., why actin forms filaments and not macrocycles). Consistent with our data, macrocycle formation is expected to be entropically favored over polymerization. However, for some proteins the nucleation−elongation mechanism is an essential part of its function. The results noted in these simple systems could be helpful for understanding the thermodynamic balance that must be achieved through evolutionary structural modifications to gain specific functions from macromolecules.

Acknowledgment. We are grateful to Prof. Stephen Sligar and Mark McLean for their assistance with the isothermal titration calorimetry. This material is based upon work supported by the U.S. Department of Energy, Division of Materials Sciences under Award DEFG02-91ER45439, through the Frederick Seitz Materials Research Laboratory at the University of Illinois at Urbana−Champaign, and by the National Science Foundation under Grant NSF CHE 03-45254.

Supporting Information Available: Detailed experimental procedures for all discussed compounds and their precursors, figure showing ^{1}H NMR data of a titration of hexamer **2** with palladium in chloroform-*d*, and raw ITC data. This material is available free of charge via the Internet at http://pubs.acs.org.

References and Notes

(1) Edelstein, S. J. *Annu. Rev. Biochem.* **1975**, *44*, 209−232.
(2) Zweifel, M. E.; Barrick, D. *Biochemistry* **2001**, *40*, 14357−14367.
(3) Koshland, D. E.; Hamadani, K. *J. Biol. Chem.* **2002**, *277*, 46841−46844.
(4) Keskin, O.; Ma, B.; Rogale, K.; Gunasekaran, K.; Nussinov, R. *Phys. Biol.* **2005**, *2*, S24−S35.
(5) Courey, A. J. *Curr. Biol.* **2001**, *11*, R250−R252.
(6) Korn, E. D. *Physiol. Rev.* **1982**, *62*, 672−737.
(7) Frieden, C. *Annu. Rev. Biochem.* **1985**, *14*, 189−210.
(8) Zhao, D.; Moore, J. S. *Org. Biomol. Chem.* **2003**, *1*, 3471−3491.
(9) Jonkheijm, P.; van der Schoot, P.; Schenning, A. P. H. J.; Meijer, E. W. *Science* **2006**, *313*, 80−83.
(10) Zimmerman, N.; Moore, J. S.; Zimmerman, S. C. *Chem. Ind.* **1998**, *15*, 604−610.
(11) Brunsveld, L.; Folmer, B. J. B.; Meijer, E. W.; Sijbesma, R. P. *Chem. Rev.* **2001**, *101*, 4071−4097.
(12) Hartgerink, J. D.; Zubarev, E. R.; Stupp, S. I. *Curr. Opin. Solid State Mater. Sci.* **2001**, *5*, 355−361.
(13) Percec, V.; Heck, J.; Johansson, G.; Tomazos, D.; Kawasumi, M. *J. Macromol. Sci., Pure Appl. Chem.* **1994**, *A31*, 1031−1070.
(14) Simic, V.; Bouteiller, L.; Jalabert, M. *J. Am. Chem. Soc.* **2003**, *125*, 13148−13154.
(15) Hirschberg, J. H. K. K.; Brunsveld, L.; Ramzi, A.; Vekemans, J. A. J. M.; Sijbesma, R. P.; Meijer, E. W. *Nature (London)* **2000**, *407*, 167−170.
(16) Wilson, A. J.; Masuda, M.; Sijbesma, R. P.; Meijer, E. W. *Angew. Chem., Int. Ed.* **2005**, *44*, 2275−2279.
(17) Chen, C.-T.; Suslisk, K. S. *Coord. Chem. Rev.* **1993**, *128*, 293−322.
(18) Archer, R. D. *Coord. Chem. Rev.* **1993**, *128*, 49−68.
(19) Paulusse, J. M. J.; Sijbesma, R. P. *Angew. Chem., Int. Ed.* **2004**, *43*, 4460−4462.
(20) Hofmeier, H.; Hoogenboom, R.; Wouters, M. E. L.; Schubert, U. S. *J. Am. Chem. Soc.* **2005**, *127*, 2913−2921.
(21) Dobrawa, R.; Würthner, F. *J. Polym. Sci., Part A* **2005**, *43*, 4981−4995.
(22) Kim, H.-J.; Zin, W.-C.; Lee, M. *J. Am. Chem. Soc.* **2004**, *126*, 7009−7014.
(23) Stone, M. T.; Moore, J. S. *J. Am. Chem. Soc.* **2005**, *127*, 5928−5935.
(24) Nelson, J. C.; Saven, J. G.; Moore, J. S.; Wolynes, P. G. *Science* **1997**, *277*, 1793−1796.
(25) Prince, R. B.; Saven, J. G.; Wolynes, P. G.; Moore, J. S. *J. Am. Chem. Soc.* **1999**, *121*, 3114−3121.
(26) Matsuda, K.; Stone, M. T.; Moore, J. S. *J. Am. Chem. Soc.* **2002**, *124*, 11836−11837.
(27) Gellman, S. H. *Acc. Chem. Res.* **1998**, *31*, 173−180.

(28) Nowick, J. S. *Acc. Chem. Res.* **1999**, *32*, 287−296.
(29) Hill, D. J.; Mio, M. J.; Prince, R. B.; Hughes, T.; Moore, J. S. *Chem. Rev.* **2001**, *101*, 3893−4011.
(30) Cubberley, M. S.; Iverson, B. L. *Curr. Opin. Chem. Biol.* **2001**, *5*, 650−653.
(31) Patch, J. A.; Barron, A. E. *Curr. Opin. Chem. Biol.* **2002**, *6*, 871−877.
(32) Sanford, A. R.; Yamato, K.; Yang, X.; Yaun, L.; Han, Y.; Gong, B. *Eur. J. Biochem.* **2004**, *271*, 1416−1425.
(33) Stone, M. T.; Heemstra, J. M.; Moore, J. S. *Acc. Chem. Res.* **2006**, *39*, 11−20.
(34) Oh, K.; Jeong, K.-S.; Moore, J. S. *Nature (London)* **2001**, *414*, 889−893.
(35) Zhao, D.; Moore, J. S. *J. Org. Chem.* **2002**, *67*, 3548−3554.
(36) Zhao, D.; Moore, J. S. *J. Am. Chem. Soc.* **2002**, *124*, 9996−9997.
(37) Zhao, D.; Moore, J. S. *J. Am. Chem. Soc.* **2003**, *125*, 16294−46299.
(38) Oh, K.; Jeong, K.-S.; Moore, J. S. *J. Org. Chem.* **2003**, *68*, 8397−8403.
(39) Flory, P. J. *Principles of Polymer Chemistry*; Cornell University Press: Ithaca, NY, 1953.
(40) Zhao, D.; Moore, J. S. *Chem. Commun.* **2003**.
(41) Zhang, W.; Moore, J. S. *J. Am. Chem. Soc.* **2005**, *127*, 11863−11870.
(42) Martin, R. B. *Chem. Rev.* **1996**, *96*, 3043−3064.
(43) Antson, A. A.; Dodson, E. J.; Dodson, G. G. *Curr. Opin. Struct. Biol.* **1996**, *6*, 142−150.
(44) Braig, K.; Otwinowski, Z.; Hegde, R.; Boisvert, D. C.; Joachimiak, A.; Horwich, A. L.; Sigler, P. B. *Nature (London)* **1994**, *371*, 578−586.
(45) Oosawa, F.; Asakura, S. *Thermodynamics of the Polymerization of Protein*; Academic Press: New York, 1975.
(46) Klug, A. *Angew. Chem., Int. Ed. Engl.* **1983**, *22*, 565−636.
(47) Hecht, S.; Khan, A. *Angew. Chem., Int. Ed.* **2003**, *42*, 6021−6024.
(48) Job, P. *Ann. Chim. Ser.* **1928**, *9*, 113−134.
(49) Harris, D. C. In *Quantitative Chemical Analysis*; 5th ed.; Freeman: New York, 2000; p 552.
(50) Though the hexamer data are also consistent with a 3:2 and a 2:3 complex, additional evidence for the 1:1 stoichiometry is provided by the isothermal titration calorimetry and MALDI MS data.
(51) Cubberley, M. S.; Iverson, B. L. *J. Am. Chem. Soc.* **2001**, *123*, 7560−7563.
(52) The theoretical description of nucleation elongation assumes that the equilibrium constant for the elongation steps is much greater than the equilibrium constant for the nucleation steps.
(53) Only the two most downfield macrocycle pyridine protons are observable in Figure 7 because the other protons are upfield of 7.8 ppm. They do have corresponding peaks but are too broadened and overlapping to be discernible.
(54) Hill, D. J.; Moore, J. S. *Proc. Natl. Acad. Sci. U.S.A.* **2002**, *99*, 5053−5057.
(55) Pazderski, L.; Szlyk, E.; Sitkowski, J.; Kamiennski, B.; Kozerski, L.; Tousek, J.; Marek, R. *Magn. Reson. Chem.* **2006**, *44*, 163−170.
(56) Lahiri, S.; Thompson, J. L.; Moore, J. S. *J. Am. Chem. Soc.* **2000**, *122*, 11315−11319.
(57) Tobe, Y.; Utsumi, N.; Kawabata, K.; Nagano, A.; Adachi, K.; Araki, S.; Sonoda, M.; Hirose, K.; Naemura, K. *J. Am. Chem. Soc.* **2002**, *124*, 5350−5364.
(58) Lin, C.-H.; Tour, J. *J. Org. Chem.* **2002**, *67*, 7761−7768.
(59) This equation, derived from ref 42, makes the following assumptions: the association constant for the addition of each macrocycle to a stack is equal, the change in chemical shift of a macrocycle is only effected by its nearest neighbors in a stack, and the chemical shift of a macrocycle at the end of the stack is the average of a free macrocycle and a fully stacked macrocycle.
(60) Stödeman, M.; Wadsö, I. *Pure Appl. Chem.* **1995**, *67*, 1059−1068.
(61) Wadsö, I. *Chem. Soc. Rev.* **1997**, 79−86.
(62) Only two (**3**) or four (**1**) nucleation events occur, and many elongation events occur.
(63) Attempts were made to obtain the molecular weight of the polymers formed. However, GPC and viscometric analysis in acetonitrile provided data from which no meaningful interpretations could be extrapolated, being neither consistent nor inconsistent with high polymer.

MA061331K